Thermodynamic Properties and Equation of State of Liquid Di-Isodecyl Phthalate at Temperature Between (273 and 423) K and at Pressures up to 140 MPa

F. Peleties [a], J. J. Segovia [b], J. P. M. Trusler [a]* and D. Vega-Maza [b]

[a.] Department of Chemical Engineering, Imperial College London, South Kensington Campus, London SW7 2AZ, United Kingdom.

[b.] Grupo de Termodinámica y Calibración (TERMOCAL), Dpto. Ingeniería Energética y Fluidomecánica, E.T.S. de Ingenieros Industriales, Universidad de Valladolid, E-47011 Valladolid, Spain

* To whom correspondence should be addressed. E-mail: m.trusler@imperial.ac.uk

Abstract

We report measurements of the thermodynamic properties of liquid di-isodecyl phthalate (DIDP) and an equation of state determined therefrom. The speed of sound in DIDP was measured at temperatures between (293.15 and 413.15) K and a pressures between (0.1 and 140) MPa with a relative uncertainty of 0.1 %. In addition, the isobaric specific heat capacity was measured at temperatures between (293.15 and 423.15) K at a pressure of 0.1 MPa with a relative uncertainty of 1 %, and the density was measured at temperatures between (273.15 and 413.15) K at a pressure of 0.1 MPa with a relative uncertainty of 0.015 %. The thermodynamic properties of DIDP were obtained from the measured speeds of sound by thermodynamic integration starting from the initial values of density and isobaric specific heat capacity obtained experimentally. The results have been represented by a new equation of state containing 9 parameters with an uncertainty in density not worse than 0.025 %. Comparisons with literature data are made.

Keywords

Density; Diisodecylphthalate; Equation of State; Isobaric Specific Heat Capacity; Sound Speed.

Introduction

Di-isodecyl phthalate (DIDP) has been proposed as an industrial standard reference liquid for the calibration of viscometers operating in the viscosity range (50 to 125) mPa·s at temperatures near 298.15 K [1; 2; 3; 4]. A review of the available data for the viscosity of DIDP at p = 0.1 MPa and at temperatures between (288.15 and 308.15) K has recently been published, together with recommended reference values at T = (293.15, 298.15 and 303.15) K [5]. DIDP may also be useful as an industrial reference fluid for the calibration of viscometers in a more extended range of temperature, and at pressures other than 0.1 MPa. With that objective in mind several groups have studied the viscosity of DIDP at elevated pressures.

In measurements of shear viscosity, it is usually necessary to know the density of the fluid in question, and a number of studies have been completed in various ranges of temperature and pressure. The objective of the present study was to determine the thermodynamic properties of DIDP in sufficiently-wide ranges of temperature and pressure to encompass likely industrial applications, including the calibration of viscosity sensors for oilfield applications. In order to obtain the density and other thermodynamic properties of the fluid at elevated pressure, we measured the speed of sound in the liquid as a function of temperature and pressure. Initial values of density and isobaric specific heat capacity were also measured as functions of temperature along the isobar at p = 0.1 MPa. Together, these measurements permitted all of the observable thermodynamic properties of the single-phase liquid to be determined in the ranges of T and p investigated.

Materials

‘‘Analysis grade” di-isodecyl phthalate was purchased from Merck with a specified mole-fraction purity > 0.998. Before use, the liquid was dried over grade 4A molecular sieves and degassed under reduced pressure. The water content was not measured. As discussed in

[5], commercially-available DIDP is a mixture of isomers having the generic structure depicted in figure 1 with varying degrees of branching in the $C_{10}H_{21}$ chains.

Octane was purchased from Fluka with a specified mole-fraction purity > 0.999 and degassed by refluxing at ambient pressure before use.

Sound-Speed Measurements

The speed of sound was measured with the dual-path pulse-echo apparatus described previously [6; 7]. Figure 2 is a cross-sectional view of the ultrasonic cell. In this apparatus, a 5 MHz thickness-mode piezoelectric disc transducer is mounted between two plane parallel reflectors positioned at distances L_1 = 20 mm and L_2 = 30 mm from the transducer. To initiate a measurement, a five-cycle tone burst with centre frequency 5 MHz and amplitude 10 V peak-to-peak was applied to the transducer causing an ultrasonic pulse to propagate through the liquid to either side of the transducer. After reflection at the end plates, echos returned to the transducer which generated an electric signal that was captured as a continuous digital record and analysed in software to obtain the difference ($t_2 - t_1$) between the round-trip times of flight on the long- and short-paths. The speed of sound u was then computed from the simple relation

$$u = 2(L_2 - L_1)/(t_2 - t_1)\,. \tag{1}$$

In this work, the pathlength difference ($L_2 - L_1$) was determined at T_0 = 298.15 K and p_0 = 0.1 MPa by means of calibration measurements in *n*-octane. The value of the speed of sound in *n*-octane at that temperature and pressure was taken to be u = 1172.0 $m \cdot s^{-1}$, the mean of the values reported in references [8; 9]. The variation of ΔL with temperature T and pressure p was calculated from the formula

$$\Delta L(T,p) = \Delta L(T_0,p_0)\left[1 + \alpha(T - T_0) - \tfrac{1}{3}\beta(p - p_0)\right] \tag{2}$$

where α = $5.5 \cdot 10^{-7}$ K^{-1} [10] is the linear thermal expansivity of quartz (assumed independent of temperature and pressure) and β is the mean isothermal compressibility of quartz at

pressures between p_0 and p. The latter was obtained from the data reported by McSkimin [11].

The speed of sound in DIDP was measured along the isotherms at T = (298.08, 313.18 333.24, 353.18, 373.10, 393.54 and 413.41) K at pressures between (0.1 and 140) MPa. However, at the two lower temperatures the greatest pressure was restricted to a lower value because the increasing viscosity of the liquid led to excessive attenuation of the ultrasound and made precise measurements of ($t_2 - t_1$) impossible above a certain pressure. One additional measurement at T = 293.06 K and p = 1.19 MPa was also made. The estimated relative uncertainty of the speed of sound is 0.1 %, and the results are given in table 1.

The experimental speed of sound were correlated by means of the implicit equation

$$(p - p_0)/p_0 = \sum_{i=1}^{3}\sum_{j=0}^{2} a_{ij}\{(u - u_0)/(\mathrm{m\cdot s^{-1}})\}^i (T/T_0)^{-j} \ . \qquad (3)$$

Here, p_0 = 0.1 MPa, T_0 = 298.15 K, and u_0 is the speed of sound at pressure p_0 which was correlated as a function of temperature as follows:

$$u_0/(\mathrm{m\cdot s^{-1}}) = \sum_{j=0}^{2} b_j (T/T_0)^{-j} \ . \qquad (4)$$

Here and elsewhere, goodness of fit is conveniently described in terms of average absolute relative deviation Δ_{AAD} and maximum absolute relative deviation Δ_{MAD} for each property. For the speed of sound, equations (3) and (4) fit the experimental data with Δ_{AAD} = 0.01 % and Δ_{MAD} = 0.03 %; the coefficients are given in table 4.

Heat Capacity Measurements

The isobaric specific heat capacity was measured in the isoperibol flow calorimeter described previously [12]. As illustrated schematically in figure 3, the calorimeter cell comprised a copper cylinder, around which the flow tube was wound and bonded with silver solder, fitted at its top end with a thermistor temperature sensor and an electric heating

element. A thermoelectric cooler (TEC) element was sandwiched between the top of the cell and the lid of the stainless-steel containment vessel, and the assembly was immersed in a temperature-controlled fluid bath. The TEC was operated at a constant current and the temperature of the cell was regulated precisely at temperature ($T - \Delta T$) , where T was the bath temperature, by operation of the heater in a proportional-integral control loop. A second electric heater fitted to the lower end of the cell was used to determine the relation between the control heater duty and the dissipated power. This calibration heater was operated in a four-wire circuit by a precision d.c. power supply with voltage and current readout. In use, the calorimeter was operated with a temperature difference ΔT = 0.5 K and at volumetric flow rates of between (2 and 5) ml·min^{-1}. In view of the high viscosity of DIDP, the fluid was driven through the calorimeter by means of a syringe pump (Isco model 100DM) instead of the isocratic HPLC pump used previously. Before each measurement, a blank run was performed with no temperature difference in order to determine the viscous dissipation in the calorimeter at each flow rate. The heat capacity was then obtained from the relation

$$c_p = (\Delta P - \Delta P')/(\dot{m}\Delta T) , \qquad (5)$$

where $\Delta P = (P_{\text{base}} - P_{\text{flow}})$ is the difference between the baseline control power without flow, P_{base}, and the control power P_{flow} during operation at mass flow rate $\dot{m}$ and temperature difference ΔT. The term $\Delta P'$ is a similarly defined change in the control heater power measured in the 'blank' run at the same flow rate but in the absence of a temperature difference.

The heat capacity of DIDP was measured at temperatures of (293.15, 313.15, 333.15, 353.15, 373.15, 393.15 and 423.15) K and the results are given in table 2. As discussed elsewhere [12; 13], the overall estimated relative uncertainty of heat capacity measurements in liquids of low viscosity is 0.35 %, and results for methylbenzene agreed with data from the literature to within ±1 %. In the present work, with a large viscosity correction to apply, the estimated overall uncertainty is enlarged to 1 %.

The results were correlated as a function of temperature by the equation

$$c_p/(\mathrm{J\cdot K^{-1}\cdot kg^{-1}}) = \sum_{j=0}^{2} c_j (T/T_0)^{-j} , \qquad (6)$$

where T_0 = 298.15 K, and the coefficients are given in table 4. Equation (6) represents the experimental heat capacities with Δ_{AAD} = 0.4 % and Δ_{MAD} = 0.8 %.

Density Measurements

Density was measured by means of the borosilicate glass pycnometer illustrated in figure 4. The bulb volume was approximately 31 mL, and a single precision-bore capillary of i.d. 2.2 mm and length 290 mm was used. A graduation mark located approximately 20 mm above the lower end of the capillary served as the reference level. After filling, the pycnometer was mounted upright in a well-stirred silicone-oil bath fitted with a narrow vertical window permitting observation of the liquid level in the capillary. The bath was controlled to ±0.01 K by means of a PID controller operating with a platinum resistance thermometer (PRT) and a 120 W heating element. In this work, a second well-stirred thermostatic bath was used for temperatures below ambient. This was an all-glass double-glazed bath filled with a mixture of water and ethanol and fitted with a cooling coil through which chilled liquid from a refrigerated-circulating bath could be passed for cooling. In either case, the temperature was measured in the bath fluid, close to the pycnometer bulb, with another PRT that had been calibrated both at the temperature of the triple point of water and against a standard PRT over the full temperature range of the measurements. The uncertainty of the measured temperature was 0.02 K. The height of the liquid meniscus above the graduation mark at the centre of the capillary was measured by means of a digital cathetometer with an uncertainty of 0.05 mm. Meniscus shape corrections were not applied but would amount to not more than 0.01 % of the total liquid volume. A difficulty with viscous liquids such as DIDP that also wet the glass is that drainage in the capillary is very slow.

Care was therefore taken to ensure that the meniscus height had reached a constant value before proceeding with the measurements.

In use, the clean and dry pycnometer was first weighted on a precision analytical balance with a resolution of 1 mg. Next, liquid was introduced by means of a syringe fitted with a 1.6 mm o.d. hypodermic of length 300 mm. Liquid could be removed, for example after initial over-filling, with a 1.6 mm o.d. PEEK tube connected through a liquid trap to a diaphragm-type vacuum pump. Once filled to the desired initial level, the pycnometer was re-weighed and the mass of liquid determined by difference, making due allowance for air buoyancy. The pycnometer was filled at the ambient temperature of approximately 295 K to a height h above the graduation mark of approximately 10 mm. The initial bath temperature was normally about 303 K. After the initial height measurement, the bath temperature was increased by about 20 K (sufficient to cause the meniscus to rise by around 150 mm) and the height re-measured. Next, liquid was sucked out of the pycnometer to return the level to approximately h = 10 mm. Since, from the second height measurement, the density at the new temperature was determined, the mass of liquid removed could also be calculated, with a relative uncertainty of about 0.001 %, from the drop in the meniscus level. Accordingly, it was not necessary to re-weigh the pycnometer after lowering the level. This process was repeated until the maximum desired temperature was reached. A second filling was required for temperatures below ambient. In this case, the initial liquid level was near to the top of the capillary and measurements proceeded downwards in temperature.

The volume of the pycnometer up to a height h above the graduation mark was calculated from the relation:

$$V = (V_0 + Ah)[1 + \alpha(T - T_0)], \tag{7}$$

where V_0 is the volume up to the graduation mark at reference temperature T_0, A is the cross-sectional area of the capillary, and α = $8.4 \cdot 10^{-6}$ K^{-1} [10] is the thermal expansivity of

the glass. The parameters V_0 and A were determined by means of calibration measurements with mercury. After use, the bulk of the liquid was first sucked out through the PEEK tube as described above. Next the pycnometer was inverted and the bulb warmed to expand the air within it thereby pushing the bulk of the remaining liquid out through the capillary. Acetone was used for rinsing and the pycnometer was finally dried under vacuum.

Considering the uncertainties of the mass, temperature and height measurements, and the neglect of capillary corrections, the overall relative uncertainty of the density was estimated to be 0.015 %.

The density of DIDP at p = 0.1 MPa was measured at various temperatures between (273 and 413) K and the results are given in table 3. The results have been correlated by means of the equation

$$\rho/(\mathrm{kg\cdot m^{-3}}) = \sum_{i=0}^{3} d_j (T/T_0)^i \,, \tag{8}$$

where T_0 = 298.15 K. The coefficients d_i are given in table 4. Equation (8) represents the experimental densities with Δ_{AAD} = 0.002 % and Δ_{MAD} = 0.004 %.

Derived Thermodynamic Properties

The thermodynamic properties of DIDP have been obtained by numerical integration of the following system of partial differential equations:

$$\left.\begin{aligned} u^{-2} &= (\partial\rho/\partial p)_T - (T/\rho^2 c_p)(\partial\rho/\partial T)_p^2 \\ (\partial c_p/\partial p)_T &= -(T/\rho^3)[2(\partial\rho/\partial T)_p^2 - \rho(\partial^2\rho/\partial T^2)_p]. \end{aligned}\right\} \tag{9}$$

The solution of equations (9) is subject to the prescribed initial conditions on $\rho(T,p)$ and $c_p(T,p)$ at $p = p_0$, and a simple predictor-corrector algorithm was used to perform the integration with step lengths δp = 0.1 MPa and δT = 10 K [6]. On each computed isobar, the

values of u, ρ and c_p were tabulated along with the isobaric thermal expansivity $\alpha = -\rho^{-1}(\partial\rho/\partial T)_p$, the isothermal compressibility $\kappa_T = \rho^{-1}(\partial\rho/\partial p)_T$, and the isochoric specific heat capacity $c_V = c_p - T\alpha^2/(\rho\kappa_T)$. Values of density obtained along selected isotherms are given in table 5, and all of the derived properties obtained are given in the supplementary data, tables S1 to S5.

The uncertainties in the derived properties were estimated from the separate contributions of uncertainties in the speeds of sound and in the initial values used. In order to quantify these contributions, we have carried out simulations in which one property at a time selected from $u(T, p)$, $\rho(T, p = p_0)$ and $c_p(T, p = p_0)$ was perturbed in a simple way consistent with its uncertainty. Incrementing all values of $u(T, p)$ by 0.1 % was found to have only a very small effect on the derived values of density, increasing in magnitude from zero at $p = p_0$ to reach approximately -0.01 % along the isobar at $p = 140$ MPa. The derived values of κ_T were changed by approximately -0.15 % at all state points, α was increased by about an amount ranging from zero at $p = p_0$ to about 0.1 % at $p = 140$ MPa, while c_p was unchanged. The principal effect of increasing $\rho(T, p = p_0)$ by 0.015 % was to increment all derived values of density by the same amount with negligible effects on κ_T, α, and c_p. Since the derived properties are sensitive to the initial values of $(\partial\rho/\partial T)_p$, we also examined the effect of a relative perturbation to $\rho(T, p = p_0)$ given by a linear function of T varying from -0.015 % at $T = 293.15$ K to 0.015 % at $T = 413.15$ K. This perturbation was found to influence the derived values of density by not more than 0.02 %, to decrease α by approximately 0.5 % at all state points, to decrease κ_T by about 0.09 % at all state points, and to have a negligible effect on c_p. Finally, increasing $c_p(T, p = p_0)$ by 1 % was found to increment all derived values of c_p by that same amount and to reduce all values of κ_T by approximately 0.12 %, with negligible effect on the other properties. Considering the combined effects of these uncertainties, we estimate that the relative uncertainties of the derived properties are 0.025 % for ρ, 0.2 % for κ_T, 0.5 % for α and 1 % for c_p. However, it is important to note that

these estimates entirely neglect the unknown effects of variation in the isomeric composition of different sample of DIDP.

The domain of integration covers the ranges 293.15 ≤ T/K ≤ 413.15 K and 0.1 ≤ p/MPa ≤ 140 and thus involves some extrapolation of the sound speed surface at the lower end of the temperature range at high pressures; however, on the basis of the uncertainty analysis discussed above, the uncertainty of the derived properties is not materially greater in this region.

Equation of State

The derived values of density are plotted along isotherms in figure 5(a) and exhibit the usual non-linear dependence upon pressure. Figure 5(b) shows the speed of sound in DIDP as a function of density, and it is striking that $u(\rho)$ is a strictly linear function along each isotherm. Figure 5(c) illustrates another interesting regularity: that $u^3(p)$ is also a strictly linear function along isotherms. In fact, the deviation of $u(\rho)$ from linearity are not worse than about 0.1 % on any isotherm, while deviations of $u^3(p)$ from linearity do not exceed 0.5 %. Eliminating u between these two linear relations, we deduce that the equation of state of the liquid must be of the form

$$\delta = (a + b\varphi)^{1/3} + c\,, \tag{10}$$

where a, b, and c are temperature-dependent parameters. Here, equation (10) is written in terms of the following reduced variables: $\varphi = p/p_0$, $\tau = (T/T_0)$ and $\delta = \rho/\rho_0$, where p_0 and T_o are a reference pressure and temperature, and ρ_0 is the density in that reference state. In the present work, p_0 = 0.1 MPa, T_0 = 298.15 K and, from equation (8), ρ_0 = 962.92 kg·m^{-3}.

In order to explore this relation further, the derived density data on each isotherm have been analysed to determine the value of the parameter c that minimises deviations from equation (10). Figure 5(d) was then plotted to confirm the linearity of $(\delta - c)^3$ as a function of reduced

pressure. Remarkably, as shown in figure 6, the parameters *a*, *b*, and *c* are nearly linear functions of temperature. We also note that *c* is always less than the liquid density at the same temperature extrapolated to the limit of zero pressure. Although the linearity of $u(\rho)$ isotherms in compressed liquids has been noted previously [14; 15], the form of equation (10) appears to be a new deduction. Additional tests carried out on data computed from high-accuracy reference equations of state [16], show that this simple equation of state holds for many liquids except close to the critical point.

Taken together with equation (6) for $c_p(T, p = p_0)$, equation (10) provides in principle a route to all of the measurable thermodynamic properties of the homogeneous liquid. The most concise and convenient way of representing this information is by integration to obtain a fundamental equation of state expressing the specific Gibbs energy *g* as a function of temperature and pressure:

$$g = \int_{T_0}^{T} c_p(T, p = p_0)dT - T\int_{T_0}^{T} c_p(T, p = p_0)d\ln T + \int_{p_0}^{p} \{\rho(T = T_0, p)\}^{-1}dp + (h_0 - Ts_0)\,. \quad (11)$$

Here, h_0 and s_0 are the specific enthalpy and the specific entropy at the reference state defined by temperature T_0 and pressure p_0. Combining equations (6), (10) and (11) we obtain

$$\begin{aligned} g = {} & c_3 T_0\{c_0(\tau - 1) - c_0\tau\ln\tau - \tfrac{1}{2}c_1(\tau^2 - 2\tau + 1) - \tfrac{1}{6}c_2(\tau^3 - 3\tau + 2)\} \\ & + (p_0/\rho_0)3b^{-1}\left[F(\tau,\varphi) - F(\tau,\varphi = 1)\right] + (h_0 - Ts_0)\,, \end{aligned} \quad (12)$$

where $c_3 = 1\ \mathrm{J\cdot kg^{-1}\cdot K^{-1}}$, and

$$F(\tau,\delta) = \left[\tfrac{1}{2}\{(a + b\varphi)^{1/3} + c\}^2 - 2c\{(a + b\varphi)^{1/3} + c\} + c^2\ln\{(a + b\varphi)^{1/3} + c\}\right]. \quad (13)$$

Expressions for all of the thermodynamic properties of the liquid may then be obtained by differentiation of this fundamental equation as detailed in the appendix.

Having obtained initial values of *a*, *b* and *c* by analysis of the derived $p\rho T$ data on each isotherm, it was conclude that the precise temperature dependence of each was quadratic:

$$\left.\begin{aligned} a &= e_1 + e_2\tau + e_3\tau^2 \\ b &= e_4 + e_5\tau + e_6\tau^2 \\ c &= e_7 + e_8\tau + e_9\tau^2 \end{aligned}\right\}. \qquad (14)$$

Initial values of the 9 parameters in equation (14) were estimated from the isothermal fits and we then proceeded to a final step in which these parameters were fine tuned to provide the best possible description of the original experimental data: *i.e.* the experimental densities at p = 0.1 MPa and the experimental $u(T,p)$ surface. In this analysis the objective function S to be minimised was defined by

$$S = N_1^{-1}\sum_{i=1}^{N_1}\{(\rho_i - \rho_{i,\mathrm{fit}})/\sigma_\rho\}^2 + N_2^{-1}\sum_{i=1}^{N_2}\{(u_i - u_{i,\mathrm{fit}})/\sigma_u\}^2 , \qquad (15)$$

where N_1 is the number of density points considered, N_2 is the number of sound-speed points, σ_ρ and σ_u are the estimated uncertainties of ρ and u respectively, and subscript 'fit' denotes properties computed from the equation of state. The optimal values obtained for the parameters e_i for i = (1 to 9) are given in table 4. In this analysis, the parameters c_0, c_1 and c_2 were not re-adjusted as they already provided an optimal description of the isobaric specific heat capacity.

The final equation of state provides an excellent representation of both the original experimental data and the derived properties obtained by thermodynamic integration. For the density at p = 0.1 MPa, Δ_{AAD} and Δ_{MAD} were identical to the values obtained with equation (8), while for $u(T,p)$ we obtained Δ_{AAD} = 0.03 % and Δ_{MAD} = 0.13 %. The equation of state represents the properties obtained by thermodynamic integration with Δ_{AAD} of 0.001 % for density, 0.06 % for isobaric thermal expansivity, 0.05 % for isothermal compressibility and 0.003 % for isobaric specific heat capacity. Thus the equation of state faithfully reproduces all properties of DIDP considered in the temperature range (293.15 to 413.15) K at pressures up to 140 MPa, and the uncertainties of the properties given by this equation are essentially the same as those of the same properties determined by thermodynamic integration.

Discussion

Several groups have reported densities of compressed liquid DIDP measured with vibrating u-tube densimeters, and the results are compared with the present equation of state in figure 7. Paredes *et al*. [17] studied three different samples of DIDP, including an aliquot of the material used in the present study, at temperatures between (283.15 and 373.15) K and at pressures up to 70 MPa. No significant differences in the density were noted between the different samples and the results for the same material as used in this study are shown as deviation from equation (10) in figure 7. The deviations are mostly with ±0.04 % and none fall outside a band of ±0.09 %. The densities reported by Harris and Bair [4] for their sample B (having the highest purity) are also in good agreement with the present results, exhibiting deviations not wore than 0.12 %. Finally, the data of Al Motari *et al*. are lower than the present results by about 0.3 % but this deviation is equal to the uncertainty stated by the authors [18]. The sample studied in [18] contained water with mass fraction $417 \cdot 10^{-6}$; however, the additional measurements at ambient pressure on dehydrated material reported in [18] imply that the observed deviations from equation (10) cannot be ascribed to water as an impurity.

Although the equation of state was determined here in the temperature range (293 to 413) K, equation (8) for the density at p = 0.1 MPa is valid at temperatures down to 273 K. Evaluating equation (10) at p = 0.1 MPa for temperatures in the range (273 to 293) K we find values that do not deviate from equation (8) by more than 0.001 %. In view of this, and of the simple nearly-linear temperature dependencies of a, b and c, it is possible that our equation of state will give useful results at temperatures down to 273 K. This assertion is partially supported by the comparison with the results of Paredes *et al*. at T = 283.15 K and $p \leq$ 70 MPa included in figure 7 [17]. A further indication comes from additional thermodynamic integration carried out in the extended temperature range (273 to 413) K employing the

correlations established for $u(T,p)$ and for $\rho(T, p = 0.1\ \text{MPa})$ and $c_p(T, p = 0.1\ \text{MPa})$. The densities estimated in that way were found to agree with those predicted by the equation of state to within 0.004 % in the worst case, which was at $T = 273$ K and $p = 140$ MPa.

A number of authors have also reported densities of DIDP at $p = 0.1$ MPa at various temperatures between (273.15 and 363.15) K [4; 19; 20], and again each used a vibrating u-tube densimeter. The results from these three literature sources, together with our own data, are shown in figure 8 as deviations from equation (8); the reference values recommended in [5] are also shown. All of the data agree very closely at temperatures near 300 K. At other temperatures, the data measured in u-tube densimeters are all mutually consistent but there are small systematic differences from the present results that are just smaller than the combined uncertainties.

As far as we are aware, the heat capacities of DIDP have not previously been reported. The present values for c_p and c_V are shown as functions of pressure and density respectively in figures 9 (a) and (b). We note that the dependence of c_p upon pressure is especially weak and is actually less than the 1 % overall relative uncertainty ascribed to that property. This weak dependence of course implies that the second temperature derivative of the specific volume is extremely small over the ranges of temperature and pressure investigated. The isochoric heat capacity is also a weak function of pressure, increasing by, at most, 2 % between $p = 0.1$ MPa and $p = 140$ MPa. Figures 9 (c) and (d) show the derivative properties κ_T and α determined in this work. The compressibility declines rapidly over the pressure range investigated, and increases rapidly with increasing temperature along an isobar; however κ_T is found to decrease with temperature at constant density. We also note that the isotherms for $\alpha(p)$ cross at a pressure of 38 MPa where $\alpha = (6.44 \pm 0.01)\cdot 10^{-4}\ \text{K}^{-1}$.

It seems likely that the form of the equation of state adopted here, either equation (10) for the density or, equivalently, equation (11) for the Gibbs energy, will be useful for other

liquids, especially substances of low volatility where a description of the vapour phase may not be required. The accuracy of the equation appears to be excellent for the sample of DIDP actually studied in this work but, as noted above, commercially-available DIDP is not isomerically pure. Consequently, the thermodynamic properties of DIDP obtained from other sources may deviate from the equation of state to a greater extent than do our own data.

In summary, the present work yields comprehensive and thermodynamically-consistent values of the thermodynamic properties of liquid DIDP in extended ranges of temperature and pressure. The results are represented accurately by the combination of a nine-parameter thermal equation of state and a three parameter correlation of the isobaric specific heat capacity, which combine to yield a 12-parameter fundamental equation of state for the liquid.

Acknowledgement

This work was supported in part by Schlumberger Cambridge Research and by the Royal Academy of Engineering.

Appendix: Derivative of the Equation of State

Equations (11) and (12) for the specific Gibbs energy may be written

$$g = g_1 + g_2 + (h_0 - Ts_0)\,, \tag{A1}$$

where

$$g_1 = c_3 T_0 \{c_0(\tau - 1) - \tfrac{1}{2}c_1(\tau^2 - 2\tau + 1) - \tfrac{1}{6}c_2(\tau^3 - 3\tau + 2) - c_0\tau \ln\tau\}\,, \tag{A2}$$

$$g_2 = (p_0 / \rho_0)3b^{-1}\left[\mathrm{F}(\delta) - \mathrm{F}(\delta_0)\right], \tag{A3}$$

δ_0 is the value of δ evaluated at $p = p_0$ (or $\varphi = 1$), and $\mathrm{F}(\delta)$ is a function defined by:

$$\mathrm{F}(\delta) = \left[\tfrac{1}{2}\delta^2 - 2c\delta + c^2 \ln\delta\right]. \tag{A4}$$

The first two temperature derivatives of g_1 are

$$c_0^{-1}(\partial g_1 / \partial T)_p = -c_0 \ln\tau - c_1(\tau - 1) - \tfrac{1}{2}c_2(\tau^2 - 1)\,, \tag{A5}$$

and

$$(c_3 T_0)^{-1}(\partial^2 g_1 / \partial T^2)_p = -c_0\tau^{-1} - c_1 - c_2\tau\,. \tag{A6}$$

The first two temperature derivatives of g_2 are

$$(\partial g_2 / \partial T)_p = \{p_0 / (T_0\rho_0)\}\left[-3b^{-2}b'\{\mathrm{F}(\delta) - \mathrm{F}(\delta_0)\} + 3b^{-1}\{\mathrm{F}_1(\delta) - \mathrm{F}_1(\delta_0)\}\right], \tag{A7}$$

and

$$\begin{aligned}(\partial^2 g_2 / \partial T^2)_p = \{p_0 / (T_0^2\rho_0)\}\big[&\{6b^{-3}(b')^2 - 3b^{-2}b''\}\{\mathrm{F}(\delta) - \mathrm{F}(\delta_0)\} \\ &- 6b^{-2}b'\{\mathrm{F}_1(\delta) - \mathrm{F}_1(\delta_0)\} + 3b^{-1}\{\mathrm{F}_2(\delta) - \mathrm{F}_2(\delta_0)\}\big],\end{aligned} \tag{A8}$$

where primes denote differentiation with respect to reduced temperature τ and $\mathrm{F}_n(\delta)$ is the nth partial derivative of $\mathrm{F}(\delta)$ with respect to τ at constant φ. These partial derivatives are given by

$$\mathrm{F}_1(\delta) = 2c'(c\ln\delta - \delta) + (\delta - 2c + c^2\delta^{-1})(\partial\delta / \partial\tau)_\varphi\,, \tag{A9}$$

and

$$\begin{aligned} \mathrm{F}_2(\delta) = {} & 2c''(c\ln\delta - \delta) + 2(c')^2\ln\delta + 4c'(c\delta^{-1} - 1)(\partial\delta/\partial\tau)_\varphi \\ & + (1 - c^2\delta^{-2})(\partial\delta/\partial\tau)_\varphi^2 + (\delta - 2c + c^2\delta^{-1})(\partial^2\delta/\partial\tau^2)_\varphi . \end{aligned} \tag{A10}$$

The partial derivative of g with respect to p of course gives $\rho^{-1} = (\rho_0\delta)^{-1}$ but equation (10) gives δ explicitly and the following useful partial derivatives may be obtained directly from that equation:

$$(\partial\delta/\partial\tau)_\varphi = c' + \tfrac{1}{3}(a + b\varphi)^{-2/3}(a' + b''\varphi) . \tag{A11}$$

$$(\partial^2\delta/\partial\tau^2)_\varphi = c'' - \tfrac{2}{9}(a + b\varphi)^{-5/3}(a' + b'\varphi)^2 + \tfrac{1}{3}(a + b\varphi)^{-2/3}(a'' + b''\varphi) . \tag{A12}$$

$$(\partial\delta/\partial\varphi)_\tau = \tfrac{1}{3}(a + b\varphi)^{-2/3} b . \tag{A13}$$

The relevant thermodynamic properties of the fluid are therefore given by:

$$\begin{aligned} s - s_0 = {} & c_3\left[c_0\ln\tau + c_1(\tau - 1) + \tfrac{1}{2}c_2(\tau^2 - 1)\right] + \\ & \{p_0/(T_0\rho_0)\}\left[3b^{-2}b'\{\mathrm{F}(\delta) - \mathrm{F}(\delta_0)\} - 3b^{-1}\{\mathrm{F}_1(\delta) - \mathrm{F}_1(\delta_0)\}\right] \end{aligned} \tag{A14}$$

$$\begin{aligned} h - h_0 = {} & c_3T_0\left[c_0(\tau - 1) + \tfrac{1}{2}c_1(\tau^2 - 1) + \tfrac{1}{3}c_2(\tau^3 - 1)\right] + \\ & (p_0/\rho_0)\left[3b^{-1}(1 + b^{-1}\tau b')\{\mathrm{F}(\delta) - \mathrm{F}(\delta_0)\} - 3b^{-1}\tau\{\mathrm{F}_1(\delta) - \mathrm{F}_1(\delta_0)\}\right] \end{aligned} \tag{A15}$$

$$\begin{aligned} c_p = {} & c_3(c_0 + c_1\tau + c_2\tau^2) - \{p_0\tau/(T_0\rho_0)\}\left[\{6b^{-3}(b')^2 - 3b^{-2}b''\}\{\mathrm{F}(\delta) - \mathrm{F}(\delta_0)\}\right. \\ & \left. - 6b^{-2}b'\{\mathrm{F}_1(\delta) - \mathrm{F}_1(\delta_0)\} + 3b^{-1}\{\mathrm{F}_2(\delta) - \mathrm{F}_2(\delta_0)\}\right] \end{aligned} \tag{A16}$$

$$\alpha = -\left[c' + \tfrac{1}{3}(a + b\varphi)^{-2/3}(a' + b''\varphi)\right]\left[T_0\{c + (a + b\varphi)^{1/3}\}\right]^{-1} \tag{A17}$$

$$\kappa_T = \left[(a + b\varphi)^{-2/3} b\right]\left[3p_0\{c + (a + b\varphi)^{1/3}\}\right]^{-1} . \tag{A18}$$

References

[1] F.J.P. Caetano, J.M.N.A. Fareleira, A.C. Fernandes, C.M.B.P. Oliveira, A.P. Serro, I.M.S. de Almeida, W.A. Wakeham, Fluid Phase Equilib. 245 (2006) 1-5.

[2] F.J.P. Caetano, J.M.N.A. Fareleira, C.M.B.P. Oliveira, W.A. Wakeham, Int. J. Thermophys. 25 (2004) 1311-1322.

[3] F.J.P. Caetano, J.M.N.A. Fareleira, C.M.B.P. Oliveira, W.A. Wakeham, J. Chem. Eng. Data 50 (2005) 1875-1878.

[4] K.R. Harris, S. Bair, J. Chem. Eng. Data 52 (2007) 272-278.

[5] F.J.P. Caetano, J.M.N.A. Fareleira, A.P. Froba, K.R. Harris, A. Leipertz, C.M.B.P. Oliveira, J.P.M. Trusler, W.A. Wakeham, J. Chem. Eng. Data 53 (2008) 2003-2011.

[6] M.J. Davila, J.P.M. Trusler, J. Chem. Thermodyn. 41 (2009) 35-45.

[7] S.J. Ball, J.P.M. Trusler, Int. J. Thermophys. 22 (2001) 427-443.

[8] G.C. Benson, Y.P. Handa, J. Chem. Thermodyn. 13 (1981) 887-896.

[9] G. Tardajos, M.D. Pena, E. Aicart, J. Chem. Thermodyn. 18 (1986) 683-689.

[10] G.W.C. Kaye, T.H. Laby, Tables of Physical and Chemical Constants, 15th ed., Longman, London, 1986.

[11] H.J. McSkimin, Journal of the Acoustical Society of America 30 (1958) 314-318.

[12] J.J. Segovia, D. Vega-Maza, C.R. Chamorro, M.C. Martin, J. Supercrit. Fluids 46 (2008) 258-264.

[13] D. Vega-Maza, Thermodynamic characterization of new generation liquid fuels with renewable components using a new high pressure isobaric calorimeter and volumetric measurements, Universidad de Valladolid, Valladolid, 2009.

[14] J.L. Daridon, A. Lagrabette, B. Lagourette, The Journal of Chemical Thermodynamics 30 (1998) 607-623.

[15] V. Kozhevnikov, Fluid Phase Equilib. 185 (2001) 315-325.

[16] E.W. Lemmon, M.O. McLinden, D.G. Friend, NIST Standard Reference Database Number 69: Thermophysical Properties of Fluid Systems, National Institute of Standards and Technology. http://webbook.nist.gov/chemistry/

[17] X. Paredes, O. Fandiño, M.J.P. Comuñas, A.S. Pensado, J. Fernández, J. Chem. Thermodyn. 41 (2009) 1007-1015.

[18] M.M. Al Motari, M.E. Kandil, K.N. Marsh, A.R.H. Goodwin, J. Chem. Eng. Data 52 (2007) 1233-1239.

[19] F.J.P. Caetano, J. Fareleira, C. Oliveira, W.A. Wakeham, J. Chem. Eng. Data 50 (2005) 1875-1878.

[20] A.P. Fröba, A. Leipertz, J. Chem. Eng. Data 52 (2007) 1803-1810.

Table 1. Speeds of sound u in DIDP at temperatures T and pressures p.

p/MPa	u/(m·s^{-1})	p/MPa	u/(m·s^{-1})	p/MPa	u/(m·s^{-1})
T = 293.06 K		T = 333.24 K		T = 373.10 K	
1.185	1436.6	90.48	1649.2	90.06	1557.2
		105.43	1694.0	100.44	1590.2
T = 298.08 K		120.28	1736.3	110.26	1620.7
1.10	1419.9	139.66	1788.5	120.18	1649.7
5.40	1439.0	1.10	1304.1	130.57	1679.6
10.18	1459.7			140.30	1707.0
16.98	1488.0	T = 353.18 K		1.35	1184.4
25.56	1522.0	1.01	1241.9		
32.76	1549.3	10.06	1288.5	T = 393.54 K	
40.15	1576.5	19.83	1335.3	1.28	1125.4
47.80	1602.9	29.89	1380.3	14.94	1203.3
55.51	1629.7	40.17	1423.1	29.73	1277.1
62.35	1652.4	50.23	1462.7	44.51	1343.3
		60.35	1500.4	59.69	1404.8
T = 313.18 K		70.31	1535.6	75.01	1462.0
1.05	1367.8	80.17	1569.0	104.93	1563.0
15.41	1432.5	90.02	1601.0	122.45	1616.7
29.86	1491.8	104.64	1646.0	139.77	1666.6
44.86	1548.5	122.12	1697.1	1.24	1125.2
60.37	1602.9	139.45	1745.0		
75.51	1652.4	1.28	1243.1	T = 413.41 K	
89.97	1697.0			1.11	1069.6
105.66	1742.8	T = 373.10 K		14.80	1152.3
119.95	1782.4	0.46	1179.1	29.64	1229.8
1.11	1367.9	1.15	1183.1	45.07	1301.7
		10.37	1233.7	60.27	1365.4
T = 333.24 K		20.03	1282.4	75.54	1423.9
1.13	1304.1	29.93	1328.6	90.15	1476.0
14.91	1370.1	40.30	1373.8	105.15	1526.0
29.76	1434.3	50.05	1413.5	119.72	1571.9
45.00	1494.4	60.04	1452.0	139.51	1630.3
60.58	1551.1	70.06	1488.7	1.13	1069.8
75.55	1601.7	80.05	1523.7		

Table 2. Isobaric specific heat capacity c_p of DIDP at p = 0.1 MPa and temperatures T.

T/K	c_p/(J·K^{-1}·kg^{-1})	T/K	c_p/(J·K^{-1}·kg^{-1})
293.15	1690	373.15	2001
313.15	1766	393.15	2047
333.15	1828	423.15	2197
353.15	1908		

Table 3. Densities ρ of DIDP at p = 0.1 MPa and temperatures T.

T/K	ρ/(kg·m^{-3})	T/K	ρ/(kg·m^{-3})
273.84	980.22	313.27	952.21
274.06	980.07	313.27	952.15
274.07	980.08	333.28	937.93
274.35	979.86	353.29	923.76
282.95	973.75	373.29	909.62
298.25	962.88	393.31	895.47
298.28	962.83	413.33	881.29
305.26	957.83		

Table 4. Coefficients in equations (3), (4), (6), (8) and (14).

$a_{10} = -1.2930$	$a_{11} = 4.9023$	$a_{12} = -1.4152$
$a_{20} = 5.7793 \cdot 10^{-4}$	$a_{21} = 1.6998 \cdot 10^{-3}$	$a_{22} = -5.5262 \cdot 10^{-4}$
$a_{30} = 1.5387 \cdot 10^{-7}$	$a_{31} = 9.3101 \cdot 10^{-8}$	$a_{32} = 1.2051 \cdot 10^{-7}$
$b_0 = 2.7022 \cdot 10^{3}$	$b_1 = -1.5598 \cdot 10^{3}$	$b_2 = 2.7239 \cdot 10^{2}$
$c_0 = 1.010 \cdot 10^{3}$	$c_1 = 3.817 \cdot 10^{2}$	$c_2 = 3.177 \cdot 10^{2}$
$d_0 = 1.17934 \cdot 10^{3}$	$d_1 = -2.22161 \cdot 10^{2}$	$d_2 = 7.20071$
$d_3 = -1.45990$		
$e_1 = 1.3157 \cdot 10^{-2}$	$e_2 = -8.2784 \cdot 10^{-3}$	$e_3 = 1.3127 \cdot 10^{-3}$
$e_4 = 3.1083 \cdot 10^{-6}$	$e_5 = 1.7545 \cdot 10^{-6}$	$e_6 = 1.3873 \cdot 10^{-6}$
$e_7 = 9.8767 \cdot 10^{-1}$	$e_8 = -1.7814 \cdot 10^{-1}$	$e_8 = 6.7883 \cdot 10^{-3}$

Table 5. Density ρ of DIDP at temperatures T and pressures p.

p/MPa	ρ/(kg·m^{-3})				
	T = 293.15 K	T = 323.15 K	T = 353.15 K	T = 383.15 K	T = 413.15 K
0.1	966.5	945.2	923.9	902.6	881.4
20	977.4	957.5	937.8	918.5	899.4
40	987.2	968.4	950.0	932.0	914.3
60	996.1	978.2	960.8	943.8	927.2
80	1004.3	987.2	970.6	954.3	938.6
100	1011.9	995.5	979.5	964.0	948.9
120	1019.1	1003.2	987.8	972.8	958.3
140	1025.8	1010.4	995.5	981.0	967.0

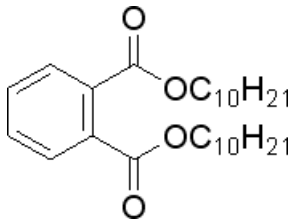

Figure 1. Structure of di-isodecyl phthalate (DIDP)

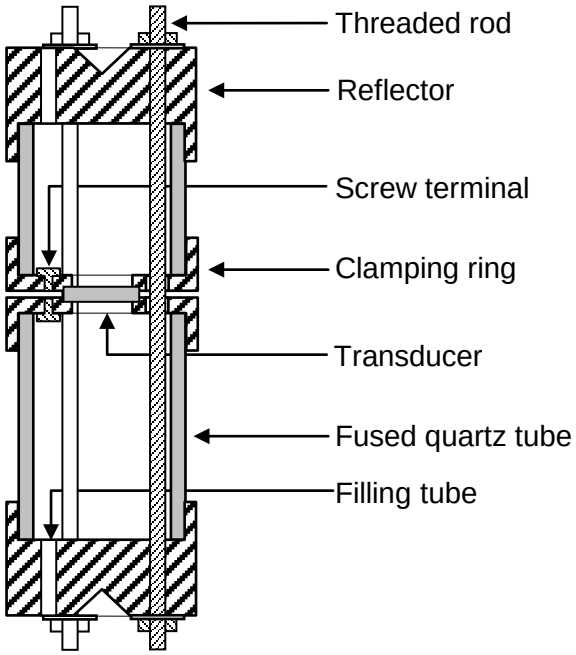

Figure 2. Cross-sectional view of the ultrasonic cell

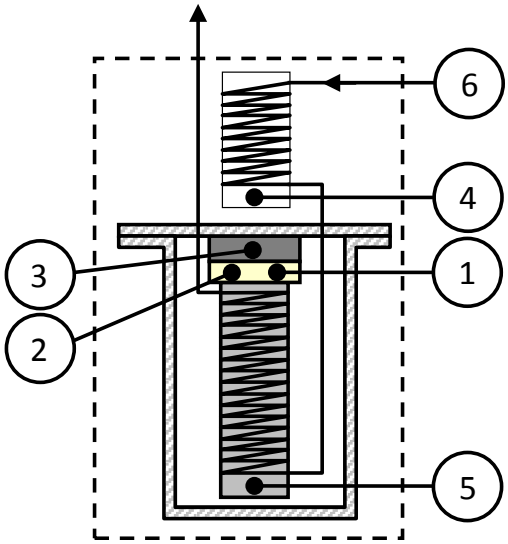

Figure 3. Schematic diagram of the flow calorimeter: 1, control heater; 2, control thermistor; 3, thermoelectric cooler; 4, pre-heater coil and bath thermometer; 5, calibration heater; 6, liquid inlet.

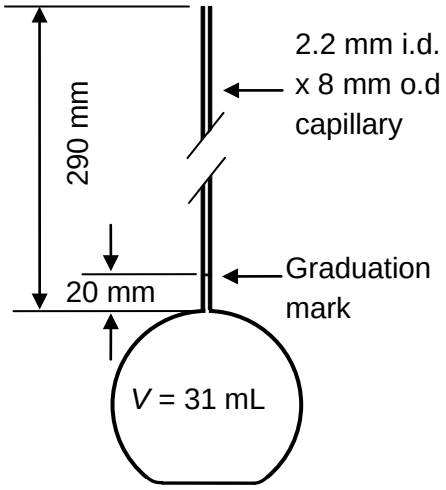

Figure 4. Borosilicate glass pycnometer

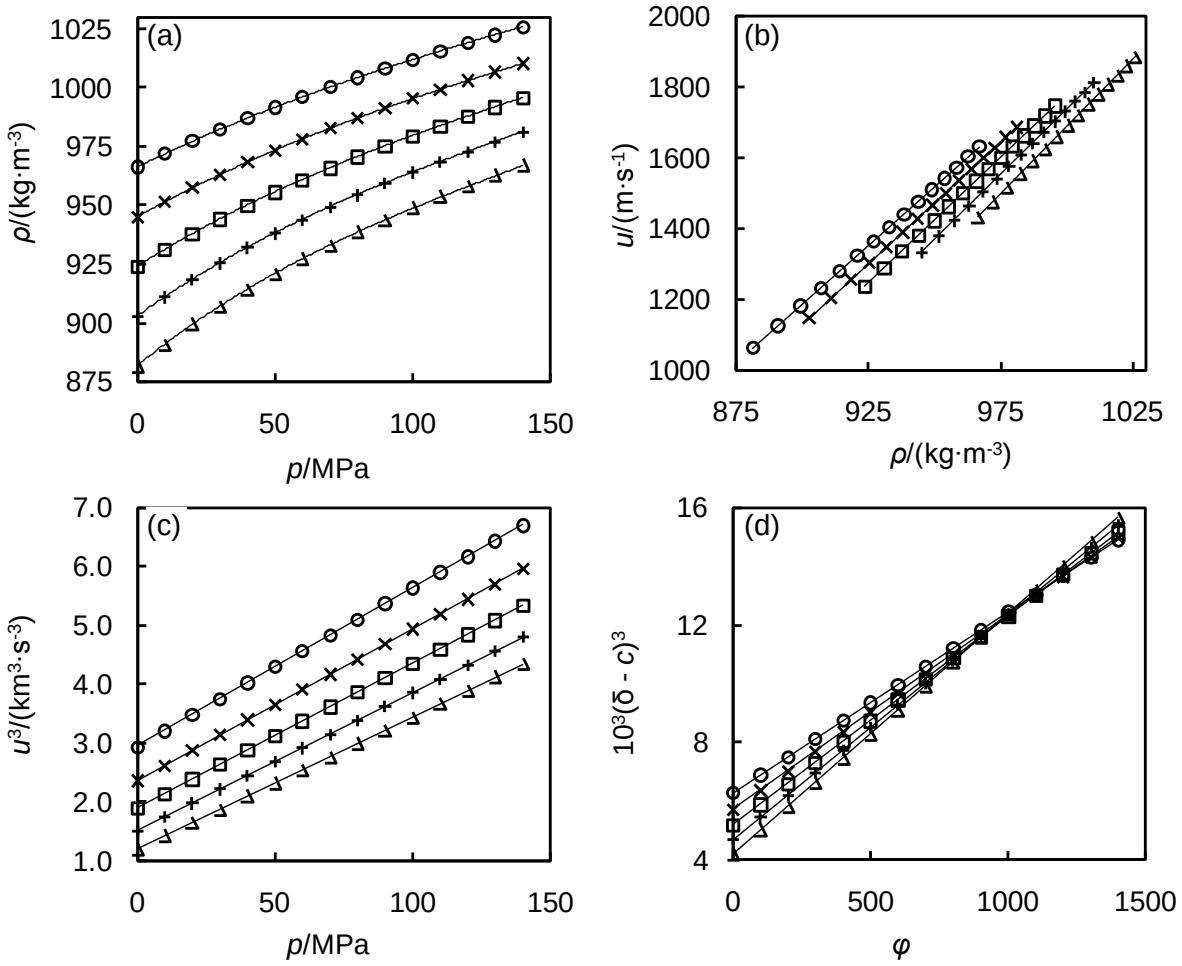

Figure 5. Density and sound speed of DIDP along isotherms. (a) density ρ as a function of pressure p; (b) sound speed u as a function of ρ; (c) u^3 as a function of p; (d) $(\delta - c)^3$ as function of reduced pressure φ. Symbols: ○, T = 293.15 K; ×, T = 323.15 K; □, T = 353.15 K; +, T = 383.15 K; △, T = 413.15 K. Lines are computed from the final equation of state.

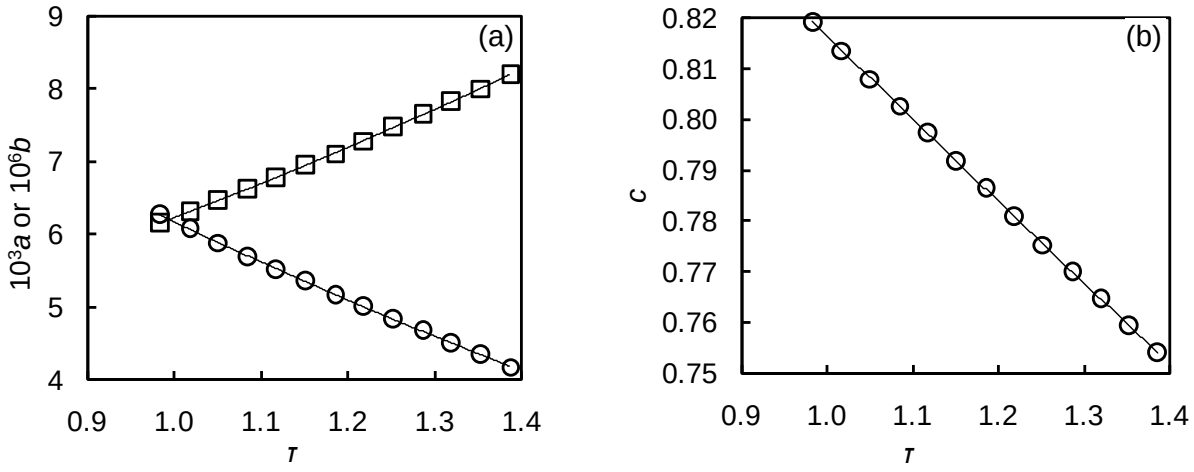

Figure 6. Parameters in equation (10) determined at reduced temperatures τ: (a) ○, a; □, b; (b) ○, c. The lines are quadratic fits.

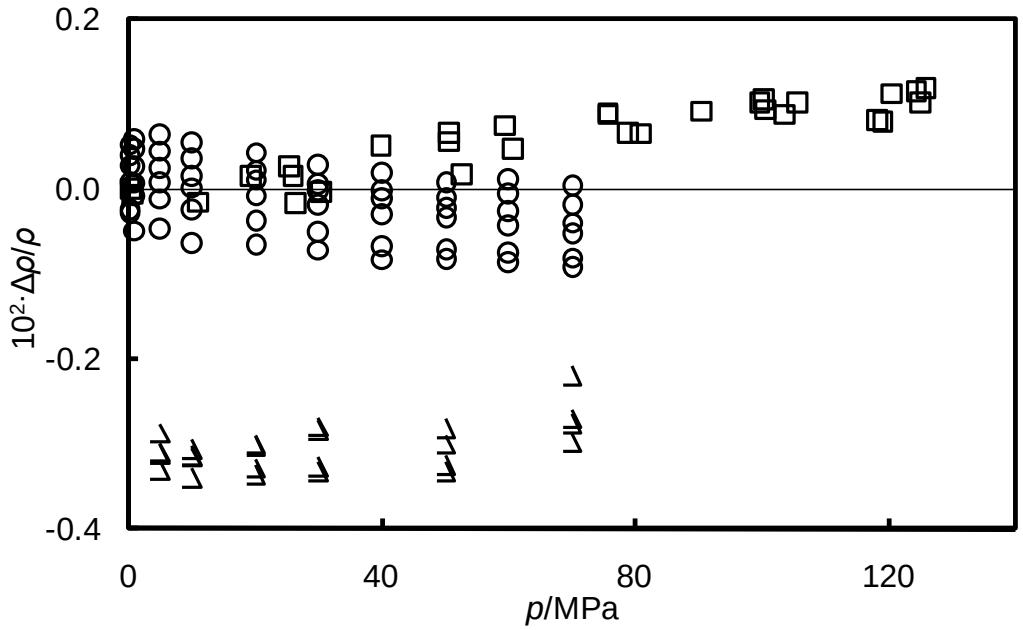

Figure 7. Comparison of literature data for the density of compressed liquid DIDP with the equation of state obtained in the present work: ○,Paredes *et al*. ; □, Harris and Bair [4]; △, Al Motari *et al*., .; ————, equation (11).

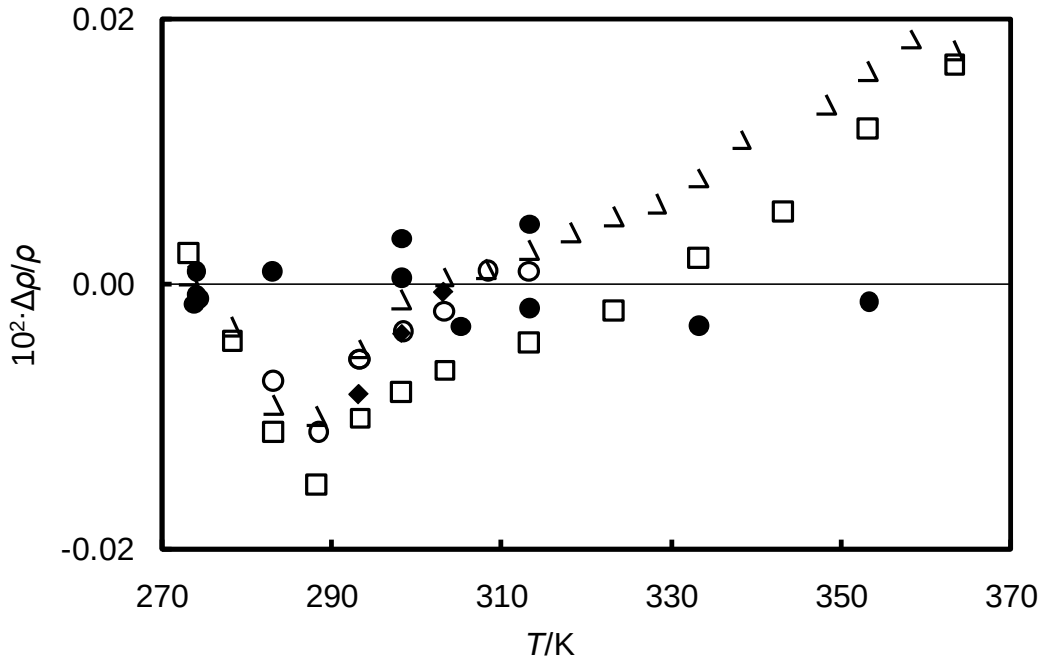

Figure 8. Relative deviations $\Delta\rho/\rho$ of experimental densities of DIDP at p = 0.1 MPa from equation (8) as function of temperature T: ●, this work; ◆, recommended reference data [5];O, Caetano *et al*. [19]; □, Harris and Bair [4]; △, Fröba and Leipertz [20].

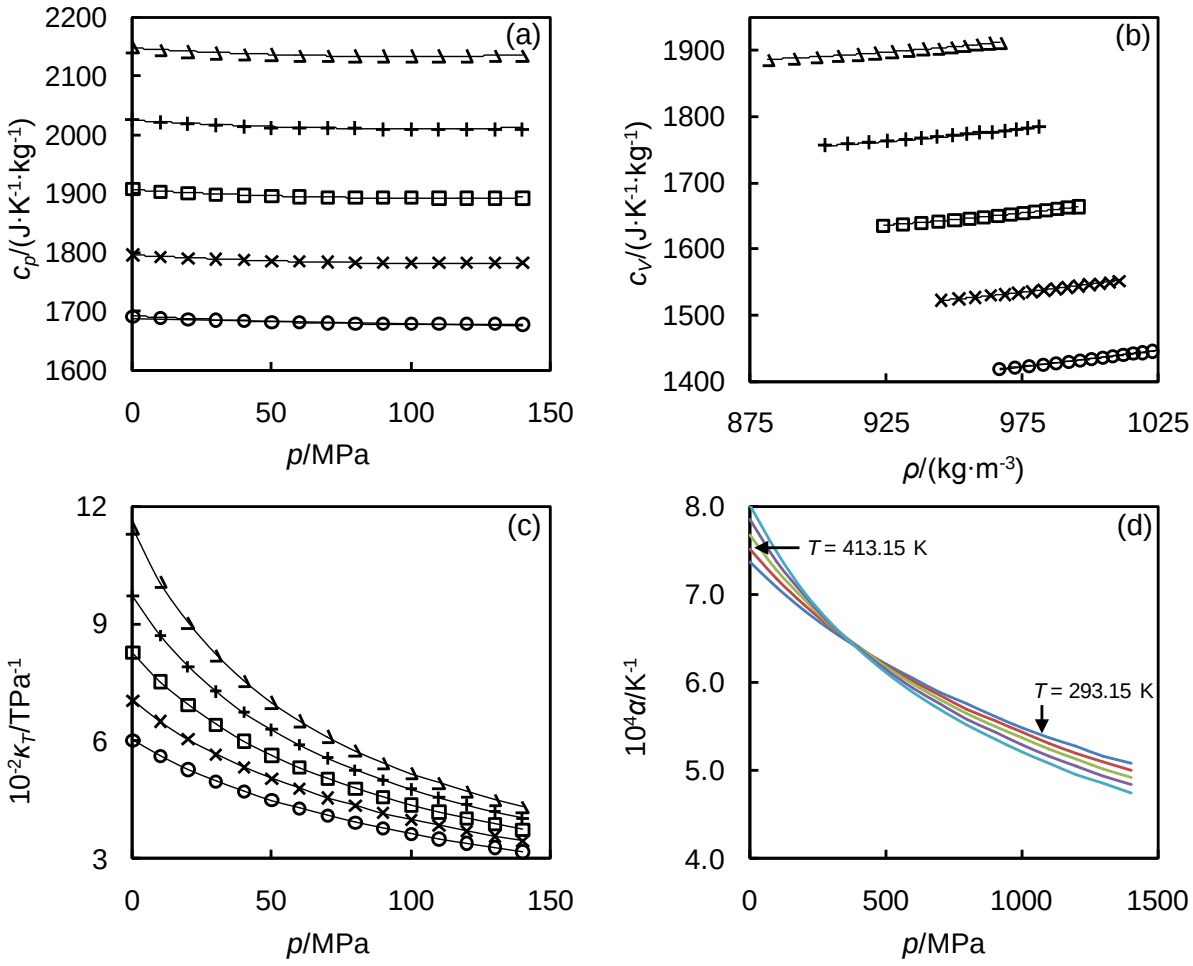

Figure 9. Derived thermodynamic properties of DIDP: (a) isobaric specific heat capacity c_p as a function of pressure p; (b) isochoric specific heat capacity c_V as a function of density ρ; (c) isothermal compressibility κ_T as a function of pressure p; (d) isobaric expansivity α as a function of pressure p. Symbols: ○, T = 293.15 K; ×, T = 323.15 K; □, T = 353.15 K; +, T = 383.15 K; △, T = 413.15 K. Symbols are suppressed in figure 9(d) to avoid obscuring the crossing point. Lines shown in (a) to (c) are computed from the final equation of state; in (d) the lines are smooth curves fitted to the data.